# EXPLOITATION OF 3D CITY MAPS FOR HYBRID 5G RTT AND GNSS POSITIONING SIMULATIONS

*José A. del Peral-Rosado*[⋆†], *Fredrik Gunnarsson*[‡], *Satyam Dwivedi*[‡], *Sara Modarres Razavi*[‡], *Olivier Renaudin*[⋆], *José A. López-Salcedo*[⋆] *and Gonzalo Seco-Granados*[⋆]

[⋆] IEEC-CERES, Universitat Autònoma de Barcelona (UAB), Bellaterra, Spain
Email: {JoseAntonio.delPeral, Olivier.Renaudin, Jose.Salcedo, Gonzalo.Seco}@uab.cat
[†] Airbus Defence and Space, Taufkirchen, Germany
[‡] Ericsson Research, Linkoping/Kista, Sweden
Email: {fredrik.gunnarsson, satyam.dwivedi, sara.modarres.razavi}@ericsson.com

**ABSTRACT**

The combination of fifth generation (5G) cellular technologies and Global Navigation Satellite Systems (GNSS) is envisaged to pave the way of fulfilling high-accuracy positioning requirements in future use cases. However, these positioning technologies are typically evaluated with independent simulations of statistical channel models for satellite and terrestrial links, which limit the applicability of the performance results. To circumvent this limitation, the proposed simulation method is based on using three-dimensional (3D) city maps to coherently determine the line-of-sight (LoS) conditions of the available satellite and cellular links. These consistent LoS measurements are then considered to assess a hybrid 5G round-trip time (RTT) and multi-constellation GNSS solution in a deep urban canyon. The combination of only one 5G RTT measurement with the GNSS observables significantly improves stand-alone GNSS solutions in terms of horizontal positioning accuracy and availability, achieving below 10 m in 80% of cases over deep urban conditions.

***Index Terms—*** 5G, GNSS, hybrid positioning, 3D city maps, deep urban canyon

## 1. INTRODUCTION

Unprecedented high-accuracy positioning requirements are envisaged for future services of fifth generation (5G) cellular systems [1]. These positioning service levels define performance requirements in terms of positioning accuracy, availability and latency, such as down to 30 cm of horizontal accuracy, 99.9% of availability and 10 ms of latency. Thus, advanced 5G positioning methods are under study in the 3rd Generation Partnership Project (3GPP) standardization. The current 5G Release 16 (Rel.16) positioning work item (WI) considers a horizontal positioning error below 10 m for 80% of user equipments (UEs) in outdoor deployment scenarios as a baseline target [2]. In this context, 5G new radio (NR) positioning methods and their hybridization with other technologies, such as Global Navigation Satellite Systems (GNSS), are analyzed in order to fulfill these baseline positioning requirements.

Standard 5G positioning methods are mainly assessed for specific deployment scenarios and evaluation methodologies, as it is described in [2]. These evaluation scenarios consider statistical 3GPP channel models specified in [3]. This standard methodology ensures the same simulation conditions for relative comparisons between different positioning methods, as in previous standards [4]. However, their simulation results are not intended to be considered as their expected positioning performance in real scenarios. As it is discussed in [5], the 3GPP channel models lack certain representativity or suitability for positioning, due to the absence of modelling of the non-line-of-sight (NLoS) bias. Furthermore, current simulations involving different positioning technologies, such as 5G- and GNSS-based methods as in [6], are performed with independent models that do not ensure a coherent scenario between these technologies.

Ray-tracing approaches are typically used to improve the channel characterization of a certain scenario, which then can be applied to design 5G network deployments as in [7] or to enhance the GNSS positioning performance as in [8–11]. However, to the best of the authors' knowledge, these approaches have not been considered for the combined study of both 5G and GNSS positioning technologies. This paper proposes a novel and simple ray-tracing approach to exploit three-dimensional (3D) city maps to coherently simulate satellite and cellular transmissions in line-of-sight (LoS) conditions. This approach is then used to assess the hybrid 5G and GNSS positioning performance in outdoor urban environments. Indeed, this study focuses only on LoS measurements in order to assess the achievable performance of standard methods, because NLoS measurements are only expected to improve the localization accuracy when exploited with advanced navigation algorithms, as in [12]. However, there is a predominance of NLoS conditions in urban environments. Thus, the use of round-trip time (RTT) measurements, even from few 5G base stations (BSs) in LoS conditions, is of high interest to enhance multi-constellation GNSS in a hybrid solution.

This paper is organised as follows. The LoS determination procedure with 3D city maps is introduced in Section 2. Hybrid 5G RTT and GNSS positioning is described in Section 3. The advantages of hybrid positioning in a deep urban canyon are discussed in Section 4, based on the proposed simulator using an example 3D city map. Finally, conclusions and future work are drawn in Section 5.

## 2. LOS DETERMINATION WITH 3D CITY MAPS

Coherent LoS satellite and cellular scenarios are here obtained with a 3D city map, in order to later assess their hybrid positioning performance. This section describes the procedure to use a 3D city map to

This work was supported in part by a Short-Term Scientific Mission (STSM) grant of COST Action CA15104 (IRACON) and by the Spanish Ministry of Science, Innovation and Universities under projects TEC2017-89925-R and TEC2017-90808-REDT and by ICREA Academia programme.

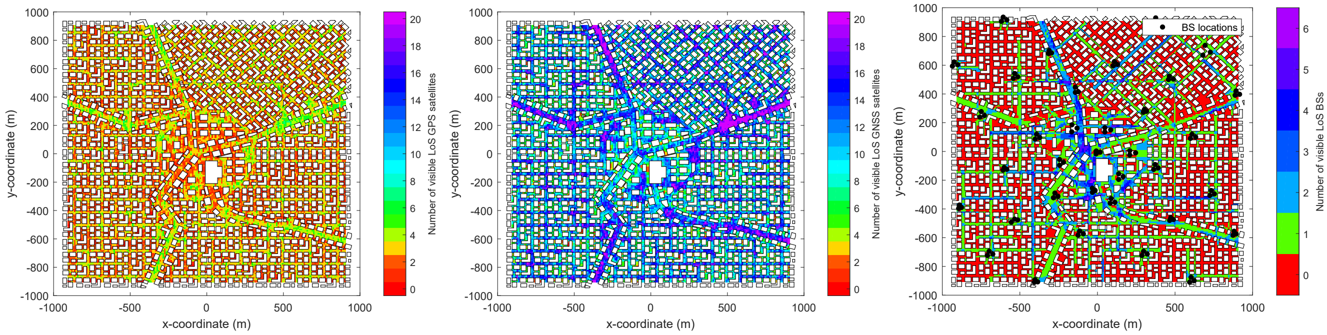


(a) GPS visibility (b) GNSS visibility (c) 5G visibility

**Fig. 1**. Visibility conditions obtained with an example 3D city map.

determine the LoS conditions between the receiver (i.e., the UE) and the transmitters, which can be either GNSS satellites or 5G BSs. An example 3D Asian city map, created by Ericsson (inspired by Tokyo and Seoul), is used to characterize a dense urban area with narrow streets and a center area with tall buildings over a 300-m radius.

### 2.1. LoS Determination Procedure

The determination of the LoS conditions between the receiver and the transmitters is here based on using a simplified ray-tracing approach over a 3D city map. The city buildings are modeled as irregular prisms with bases at the ground floor and rooftop, using a random building height between a certain interval. For a given pair of transmitter and receiver locations, i.e., GNSS satellite and UE or 5G BS and UE, their LoS vector is said to be obstructed if it intersects with at least one building face of the 3D city map. Thus, the LoS determination procedure is based on analyzing the existence of non-obstructed LoS vectors between each outdoor UE location and the available GNSS satellite and 5G BS locations. This procedure is performed with an iterative search of possible building obstructions for each LoS vector between receiver and transmitters locations.

### 2.2. GNSS Satellite Visibility

The LoS determination procedure is first exploited to analyze the GNSS satellite visibility, i.e., the number of LoS satellites for a certain UE location. For this analysis, let us consider the four main GNSS constellations with full operational capabilities, i.e., GPS with 24 satellites, Galileo with 27 satellites, GLONASS with 24 satellites and Beidou with 27 satellites. The locations of these satellites are here obtained with an orbiter simulator. The UE locations are generated by using a rectangular grid with a resolution of 10 m over an area of 3.24 km$^2$. Only outdoor UE locations are considered, resulting in 19014 UE locations. The UE height is set to 1.5 m. Given the large number of outdoor UE locations, this analysis only considers one GNSS epoch per UE location.

The GNSS satellite visibility is first assessed with a single constellation, i.e., GPS. As it is shown in Figure 1a, the dense urban area with narrow streets results in very low GPS visibility, with less than 3 LoS satellites, which is also the case for the center area with tall buildings. This situation does not allow to estimate the UE position. In contrast, the GPS visibility improves in open areas, such as in wide avenues, where the number of LoS satellites is around 5. The GNSS visibility significantly increases with multiple constellations, as it is shown in Figure 1b. In case of considering all four GNSS constellations, the number of LoS satellites is above 10 in most of the UE locations. Still, there are deep urban canyons, where even the multi-constellation GNSS visibility decreases below 3 LoS satellites. Those harsh environments, either considering single- or multi-constellation GNSS solutions, can be of interest for the application of hybrid positioning algorithms, where few 5G observables can complement GNSS observables to enhance the positioning accuracy and availability.

### 2.3. 5G BS Visibility

The 5G BS visibility is now assessed for the same 3D city map and UE locations as in the previous section. The visibility analysis of the example 5G deployment is shown in Figure 1c with three-sectorial BSs depicted by black dots. In the dense urban area, the 5G BSs are deployed above the building rooftops, i.e., BS heights between 20 and 40 m, with an inter-site distance (ISD) around 400 m. In the center area, the ISD is reduced to around 200 m with BSs above the rooftop of tall buildings, i.e., BS heights between 40 and 100 m.

According to Figure 1c, in around 42% of the UE locations there is at least one 5G BS in LoS over the dense urban area with narrow streets, while this percentage increases up to 80% in the center area thanks to the dense BS deployment. The visibility of 5G BSs increases with those BS sectors located at the building edges and/or close to street intersections. This situation can be found in the center area and in wide avenues, where the number of LoS 5G BSs can reach up to 6. However, these LoS BSs may not have a good geometry for positioning only with 5G transmissions, e.g. visible LoS BS sectors from the same site or BSs along a street. Thus, hybrid 5G and GNSS solutions are of high interest to still exploit these potentially accurate LoS 5G observables.

## 3. HYBRID 5G RTT AND GNSS POSITIONING

The lack of sufficient observables to perform either 5G or GNSS stand-alone positioning can be overcome with the combination of the available observables from both systems. This study considers the use of only LoS measurements, in order to assess the achievable positioning performance, since NLoS measurements are expected to significantly degrade the positioning accuracy. Thus, the 5G RTT and GNSS pseudorange errors in LoS conditions are assumed Gaussian-distributed with zero-mean and certain error variance. This section describes the hybrid positioning algorithm that combines 5G RTT and GNSS code pseudorange observables.

Let us first model the $k$-th 5G RTT observable in LoS as

$$\hat{\rho}_{5\mathrm{G},k} = c \cdot \hat{\tau}_{5\mathrm{G},k} = \|\mathbf{x}_{\mathrm{BS},k} - \mathbf{x}_{\mathrm{UE}}\| + e_{\mathrm{RTT},k}, \quad (1)$$

where $\hat{\tau}_{5\mathrm{G},k}$ is the one-way time-of-flight of the 5G signal, $\mathbf{x}_{\mathrm{BS},k} = [x_{\mathrm{BS},k}, y_{\mathrm{BS},k}, z_{\mathrm{BS},k}]$ is the $k$-th BS position, $\mathbf{x}_{\mathrm{UE}} = [x_{\mathrm{UE}}, y_{\mathrm{UE}}, z_{\mathrm{UE}}]$ is the UE position, $c$ is the speed of light, and $e_{\mathrm{RTT},k}$ is the RTT error, which is defined as $e_{\mathrm{RTT},k} \sim \mathcal{N}(0, \sigma^2_{\mathrm{RTT},k})$, $\sigma^2_{\mathrm{RTT},k}$ being the RTT error variance from the $k$-th BS. This error variance includes the receiver-transmitter synchronization error, noise errors, and multipath errors. Thanks to the two-way transmission between receiver and transmitter, there is no UE clock offset present in the RTT observables, which relaxes the positioning problem.

The $k$-th GNSS code pseudorange in LoS is modelled as

$$\hat{\rho}_{\mathrm{GNSS},k} = c \cdot \hat{\tau}_{\mathrm{GNSS},k} = \|\mathbf{x}_{\mathrm{sat},k} - \mathbf{x}_{\mathrm{UE}}\| + c \cdot \delta t + e_{\mathrm{sat},k}, \quad (2)$$

where $\hat{\tau}_{\mathrm{GNSS},k}$ is the time-of-flight of the GNSS signal, $\mathbf{x}_{\mathrm{sat},k} = [x_{\mathrm{sat},k}, y_{\mathrm{sat},k}, z_{\mathrm{sat},k}]$ is the $k$-th satellite position, $\delta t$ is the clock offset of the UE (referenced to a GNSS time), and $e_{\mathrm{sat},k}$ is the pseudorange error. This GNSS pseudorange error is also assumed Gaussian-distributed with zero-mean, i.e., $e_{\mathrm{sat},k} \sim \mathcal{N}(0, \sigma^2_{\mathrm{sat},k})$, where $\sigma^2_{\mathrm{sat},k}$ is the pseudorange error variance from the $k$-th satellite, which includes orbit and clock errors, residual ionosphere and troposphere errors, receiver noise errors, and multipath errors. The GNSS code pseudorange formulation in (2) is here assumed to be applicable to multiple GNSS constellations, because the inter-system clock bias is assumed to be removed with assistance information and its residual error is included in the pseudorange error $e_{\mathrm{sat},k}$.

Due to low availability of LoS observables, the UE height is assumed to be known, such as by means of a barometer. Then, the weighted least squares (WLS) solution of this trilateration problem is formulated as the nonlinear least squares (NLS) minimization

$$\hat{\boldsymbol{\theta}} = \left[\hat{x}_{\mathrm{UE}}, \hat{y}_{\mathrm{UE}}, \hat{\delta t}\right]^{\mathrm{T}} = \arg\min_{\boldsymbol{\theta}} \left\{\|\boldsymbol{\rho}(\boldsymbol{\theta}) - \hat{\boldsymbol{\rho}}\|^2_{\mathbf{W}}\right\}, \quad (3)$$

where $\boldsymbol{\rho}(\boldsymbol{\theta}) = [\rho_1(\boldsymbol{\theta}), \rho_2(\boldsymbol{\theta}), \cdots, \rho_M(\boldsymbol{\theta})]^{\mathrm{T}}$ for a total number of transmitters $M$, $\hat{\boldsymbol{\rho}} = [\hat{\rho}_1, \hat{\rho}_2, \cdots, \hat{\rho}_M]^{\mathrm{T}}$, and $\mathbf{W}$ is the diagonal weighting matrix defined as

$$\mathbf{W} = \begin{bmatrix} \mathrm{diag}\left(\mathbf{w}_{5\mathrm{G}}\right) & \mathbf{0}_{M_{\mathrm{BS}} \times M_{\mathrm{sat}}} \\ \mathbf{0}_{M_{\mathrm{sat}} \times M_{\mathrm{BS}}} & \mathrm{diag}\left(\mathbf{w}_{\mathrm{GNSS}}\right) \end{bmatrix}, \quad (4)$$

being $\mathbf{w}_{5\mathrm{G}}$ the vector of 5G RTT weighting coefficients and $\mathbf{w}_{\mathrm{GNSS}}$ the vector of GNSS weighting coefficients, which can be determined based on signal quality metrics, e.g. signal-to-noise ratio (SNR). The $M$ transmitters used for hybrid positioning is the sum of the number of visible LoS BSs, $M_{\mathrm{BS}}$, and the number of visible LoS GNSS satellites, $M_{\mathrm{sat}}$, i.e., $M = M_{\mathrm{BS}} + M_{\mathrm{sat}}$. For $1 \leq m \leq M_{\mathrm{BS}}$ corresponding to 5G RTT observables, $\mathbf{x}_m = \mathbf{x}_{\mathrm{BS},m}$, $\rho_m(\boldsymbol{\theta}) = \|\mathbf{x}_{\mathrm{BS},m} - \mathbf{x}_{\mathrm{UE}}\|$, and $\hat{\rho}_m = \hat{\rho}_{5\mathrm{G},m}$. For $M_{\mathrm{BS}} + 1 \leq m \leq M$ corresponding to the GNSS code pseudorange observables, $\mathbf{x}_m = \mathbf{x}_{\mathrm{sat},(m-M_{\mathrm{BS}})}$, $\rho_m(\boldsymbol{\theta}) = \|\mathbf{x}_m - \mathbf{x}_{\mathrm{UE}}\| + c \cdot \delta t$, and $\hat{\rho}_m = \hat{\rho}_{\mathrm{GNSS},(m-M_{\mathrm{BS}})}$. Our WLS implementation is based on the well-known iterative Gauss-Newton (GN) method. Then, the GN solution at the $\ell$-th iteration is defined as

$$\hat{\boldsymbol{\theta}}_\ell = \hat{\boldsymbol{\theta}}_{\ell-1} + \left(\mathbf{G}^{\mathrm{T}}_{\ell-1}\mathbf{W}^{-1}\mathbf{G}_{\ell-1}\right)^{-1}\mathbf{G}^{\mathrm{T}}_{\ell-1}\mathbf{W}^{-1}\left(\boldsymbol{\rho}\left(\hat{\boldsymbol{\theta}}_{\ell-1}\right) - \hat{\boldsymbol{\rho}}\right), \quad (5)$$

where the Jacobian matrix or geometry matrix of $\boldsymbol{\rho}(\hat{\boldsymbol{\theta}})$ is a $M \times 3$ matrix defined for $1 \leq m \leq M_{\mathrm{BS}}$ as

$$[\mathbf{G}]_{m,1:3} = \begin{bmatrix} \frac{x_m - \hat{x}_{\mathrm{UE}}}{\rho_m(\hat{\boldsymbol{\theta}})} & \frac{y_m - \hat{y}_{\mathrm{UE}}}{\rho_m(\hat{\boldsymbol{\theta}})} & 0 \end{bmatrix} \quad (6)$$

and defined for $M_{\mathrm{BS}} + 1 \leq m \leq M$ as

$$[\mathbf{G}]_{m,1:3} = \begin{bmatrix} \frac{x_m - \hat{x}_{\mathrm{UE}}}{\rho_m(\hat{\boldsymbol{\theta}})} & \frac{y_m - \hat{y}_{\mathrm{UE}}}{\rho_m(\hat{\boldsymbol{\theta}})} & -1 \end{bmatrix}. \quad (7)$$

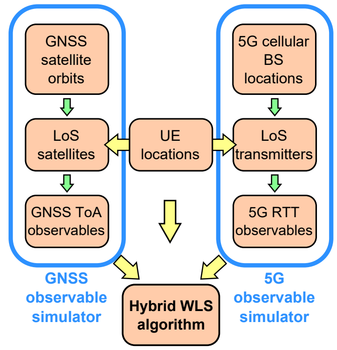


(a) Simulator architecture

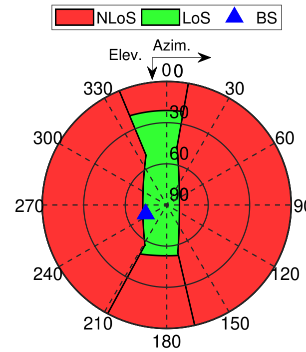


(b) Sky plot of a deep urban canyon

**Fig. 2**. Architecture of the hybrid 5G and GNSS simulator used for the positioning performance assessment over a deep urban canyon.

## 4. SIMULATION RESULTS

This section presents an analysis of the hybrid performance gains in a deep urban canyon, by using the simulator shown in Figure 2a. The lack of GNSS satellite visibility is compensated with one additional 5G RTT measurement in LoS conditions. The hybrid positioning performance is then assessed with respect to the stand-alone GNSS.

### 4.1. Deep Urban Canyon Scenario

As it is discussed in Section 2, dense urban areas with narrow streets and urban areas with tall buildings reduce significantly the GNSS visibility. Thus, the use of hybrid positioning methods is of high interest in these harsh environments. An example of deep urban canyon can be found by considering the UE position $\mathbf{x}_{\mathrm{UE}} = [-530, 550, 1.5]^{\mathrm{T}}$m within the example 3D city map. The sky plot result of this deep urban canyon is shown in Figure 2b, where the azimuth and elevation are in degrees. As it can be seen, the UE is surrounded by four buildings of different heights, and the sky area with LoS satellite conditions is very limited. In this street, there is a 5G BS at the roof edge of one of the buildings.

Given this deep urban canyon example, the GNSS visibility is analyzed for different number of constellations, by simulating full GNSS operational capabilities with satellite locations every minute over 24 hours. Considering the known user height, the maximum GNSS positioning availability is computed by summing the number of LoS GNSS satellites equal or above 3, which results in 8.06%, 76.74% and 97.71% for single-, dual- and multi-constellation GNSS solutions, respectively. This result indicates the need to use multiple GNSS constellations, in order to achieve a high positioning availability (i.e., above 95%) only using GNSS observables.

### 4.2. Hybrid Positioning Performance

The positioning performance is first assessed from a geometric perspective in this deep urban canyon scenario. The reduced sky visibility results in poor geometric conditions of the positioning problem, which leads to a poor positioning performance. This is typically assessed with the geometric dilution of precision (GDOP), defined as

$$\mathrm{GDOP} = \sqrt{\mathrm{tr}\left\{\left(\mathbf{G}^{\mathrm{T}} \cdot \mathbf{G}\right)^{-1}\right\}}. \quad (8)$$

The cumulative density function (CDF) of the GDOP is shown in Figure 3 for GNSS and hybrid positioning solutions, i.e., without or

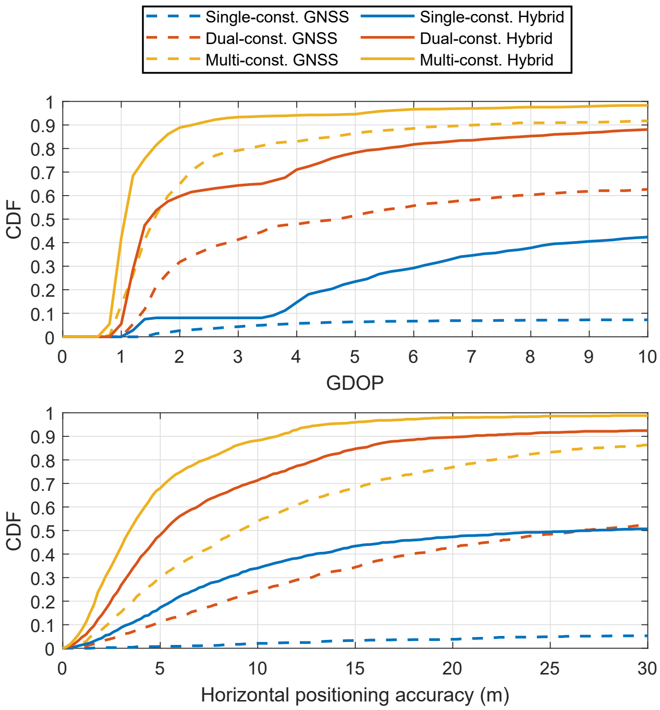


**Fig. 3**. CDF of the GDOP and horizontal positioning accuracy for GNSS stand-alone and hybrid solutions in a deep urban canyon, using only one 5G RTT observable with $\sigma_{\mathrm{RTT}} = 1$ m.

with one 5G RTT observable, respectively. The GDOP values below 2 are expected to provide precise solutions, while values above 6 are expected to lead to positioning outages due to deficient geometry. The results show the significant improvement on the GDOP when adding only one 5G RTT to the available LoS GNSS observables. The additional 5G RTT observables relaxes the constrained positioning problem, i.e., due to the reduced number of observables, and it improves the geometry in most of the epochs due to the perpendicular direction of the BS antenna with respect to the street orientation.

The positioning performance is now assessed by configuring the error variances of the tightly-coupled hybrid positioning simulator in this deep urban canyon. The standard deviation of the 5G RTT error is first set to one meter, i.e., $\sigma_{\mathrm{RTT}} = 1$ m, by taking as a reference the meter-level accuracy of WiFi fine timing measurements (FTM) in LoS conditions with 80 MHz bandwidth [13]. The GNSS code pseudorange error is obtained as a function of the satellite elevation, by using the User Equivalent Range Error (UERE) analysis and its loopup table described in [5] and [6] for dual-frequency GNSS receivers. The resulting GNSS error standard deviation is between 4 and 5 m. Using the LoS 5G and GNSS observables, the positioning algorithm is evaluated with full information of the ranging errors, i.e., by using the absolute RTT error for the 5G weighting coefficient as $\mathbf{w}_{5\mathrm{G}} = |e_{\mathrm{RTT},1}|^2$, and the absolute pseudorange errors for the GNSS weighting coefficients as $\mathbf{w}_{\mathrm{GNSS}} = \left[|e_{\mathrm{sat},1}|^2, |e_{\mathrm{sat},2}|^2, \cdots, |e_{\mathrm{sat},M_{\mathrm{sat}}}|^2\right]^{\mathrm{T}}$. This simulation approach allows to assess the performance limits of the GNSS stand-alone and hybrid solutions when adding one 5G RTT observable, while the practical design of the weighting coefficients and the strategies to achieve this performance are left for future work. As it is shown in Figure 3, the resulting horizontal positioning accuracy

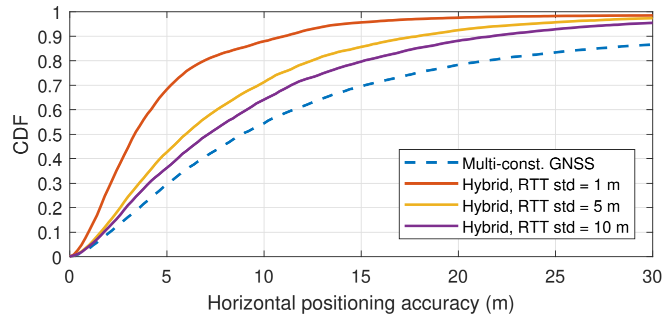


**Fig. 4**. CDF of the horizontal positioning accuracy for multi-constellation GNSS and hybrid solutions in a deep urban canyon, using only one 5G RTT observable with different $\sigma_{\mathrm{RTT}}$ values.

of the hybrid approach significantly improves the GNSS stand-alone solutions, by using only one high-accuracy 5G RTT observable. The deep urban canyon conditions certainly limit the availability of LoS satellites even with multi-constellation solutions, leading to a positioning accuracy above 20 m on the 80% of cases. Thus, the additional 5G RTT observable provides three main benefits to complement the GNSS solution, in terms of relaxation of the positioning problem, improved geometry and enhanced observable.

Let us finally assess the impact of the ranging accuracy of the additional 5G RTT observable. Considering the same GNSS conditions, the standard deviation of the 5G RTT observable $\sigma_{\mathrm{RTT}}$ is set equal to 1, 5 or 10 m. As it is shown in Figure 4, an RTT accuracy of 1 m is necessary to fulfil the 10-m positioning accuracy on the 80% of cases. Still, the additional RTT measurement enhances the positioning availability even with lower RTT accuracies, e.g. for $\sigma_{\mathrm{RTT}}$ values of 5 or 10 m, motivating the use of this hybrid approach.

## 5. CONCLUSIONS

A procedure to exploit three-dimensional (3D) city maps is proposed in this work to assess the performance gains of hybrid fifth generation (5G) round-trip time (RTT) and Global Navigation Satellite System (GNSS) positioning in a deep urban canyon. A simplified ray-tracing procedure is proposed to determine the line-of-sight (LoS) conditions of 5G and GNSS signals based on the 3D city map, instead of using independent statistical channel models. Using this procedure, the satellite and cellular visibility are analyzed, resulting in a reduced number of LoS GNSS satellites, even with multiple constellations, and in a predominance of non-LoS (NLoS) 5G links. Thus, a tightly-coupled hybrid 5G RTT and GNSS algorithm is proposed to combine the available LoS observables, by assuming the discard of NLoS observables in order to evaluate the achievable hybrid positioning performance. The simulation results over a deep urban canyon indicate that already the addition of only one 5G RTT measurement to the GNSS observables significantly improves the positioning performance. This additional 5G RTT measurement increases the positioning availability, by relaxing the positioning problem and improving its geometry, and it enhances the positioning accuracy. Still, high-accuracy 5G RTT observables with a 1-m standard deviation are necessary to be combined with multi-constellation GNSS observables in order to fulfill high-accuracy positioning requirements, i.e., a horizontal positioning accuracy of 10 m on the 80% of cases. Future work aims at studying the impact of the NLoS bias with 3D city maps, as well as the use or mitigation of NLoS or outlier observables within the hybrid positioning algorithm.

## 6. REFERENCES


[1] 3GPP TS 22.261, "Service requirements for next generation new services and markets," Rel. 16, 2019.

[2] 3GPP TR 38.855, "Study on NR positioning support," Rel. 16, 2019.

[3] 3GPP TR 38.901, "Study on channel model for frequencies from 0.5 to 100 GHz," Rel. 14, Dec. 2017.

[4] J. A. del Peral-Rosado, R. Raulefs, J. A. López-Salcedo, and G. Seco-Granados, "Survey of cellular mobile radio localization methods: From 1G to 5G," *IEEE Communications Surveys Tutorials*, vol. 20, no. 2, pp. 1124–1148, Secondquarter 2018.

[5] R1-1900236, "Performance evaluation for hybrid positioning based on GNSS and NR," 3GPP, ESA, RAN1 AH-1901, Taipei, Taiwan, 2019.

[6] J. A. del Peral-Rosado, O. Renaudin, C. Gentner, R. Raulefs, E. Domínguez-Tijero, A. Fernández-Cabezas, F. Blázquez-Luengo, G. Cueto-Felgueroso, A. Chassaigne, D. Bartlett, F. Grec, L. Ries, R. Prieto-Cerdeira, J. A. López-Salcedo, and G. Seco-Granados, "Physical-layer abstraction for hybrid GNSS and 5G positioning evaluations," in *Proc. VTC-Fall*, Sep. 2019.

[7] D. He, B. Ai, K. Guan, L. Wang, Z. Zhong, and T. Kürner, "The design and applications of high-performance ray-tracing simulation platform for 5G and beyond wireless communications: A tutorial," *IEEE Communications Surveys Tutorials*, vol. 21, no. 1, pp. 10–27, Firstquarter 2019.

[8] S. S. Saab and Z. M. Kassas, "Power matching approach for GPS coverage extension," *IEEE Transactions on Intelligent Transportation Systems*, vol. 7, no. 2, June 2006.

[9] P. D. Groves, "Shadow matching: A new GNSS positioning technique for urban canyons," *The Journal of Navigation*, vol. 64, no. 3, pp. 417–430, July 2011.

[10] J. T. Isaacs, A. T. Irish, F. Quitin, U. Madhow, and J. P. Hespanha, "Bayesian localization and mapping using GNSS SNR measurements," in *Proc. IEEE/ION PLANS*, May 2014.

[11] S. Ragothaman, M. Maaref, and Z. M. Kassas, "Multipath-optimal UAV trajectory planning for urban UAV navigation with cellular signals," in *Proc. VTC2019-Fall*, Sep. 2019.

[12] C. Gentner, T. Jost, W. Wang, S. Zhang, A. Dammann, and U. Fiebig, "Multipath assisted positioning with simultaneous localization and mapping," *IEEE Transactions on Wireless Communications*, vol. 15, no. 9, pp. 6104–6117, Sep. 2016.

[13] M. Ibrahim, H. Liu, M. Jawahar, V. Nguyen, M. Gruteser, R. Howard, B. Yu, and F. Bai, "Verification: Accuracy evaluation of WiFi fine time measurements on an open platform," in *Proc. 24th Annu. Int. Conf. Mobile Comput. Netw.*, Nov. 2018.